Lattice and magnetic structures of $PrFeAsO$, $PrFeAsO_{0.85}F_{0.15}$, and $PrFeAsO_{0.85}$

Jun Zhao,[1] Q. Huang,[2] Clarina de la Cruz,[1,3] J. W. Lynn,[2] M. D. Lumsden,[3] Z. A. Ren,[4] Jie Yang,[4] Xiaolin Shen,[4] Xiaoli Dong,[4] Zhongxian Zhao,[4] and Pengcheng Dai[1,3]

[1]*Department of Physics and Astronomy, The University of Tennessee, Knoxville, Tennessee 37996-1200, USA*

[2]*NIST Center for Neutron Research, National Institute of Standards and Technology, Gaithersburg, Maryland 20899-6012, USA*

[3]*Neutron Scattering Science Division, Oak Ridge National Laboratory, Oak Ridge, Tennessee 37831, USA*

[4]*Beijing National Laboratory for Condensed Matter Physics, Institute of Physics, Chinese Academy of Sciences, Beijing 100080, People's Republic of China*

(Received 29 July 2008; published 7 October 2008)

We use powder neutron diffraction to study the spin and lattice structures of polycrystalline samples of nonsuperconducting PrFeAsO and superconducting $PrFeAsO_{0.85}F_{0.15}$ and $PrFeAsO_{0.85}$. We find that PrFeAsO exhibits abrupt structural phase transitions at 153 K followed by static long-range antiferromagnetic order at 127 K. Both the structural distortion and magnetic order are similar to other rare-earth oxypnictides. Electron doping the system with either fluorine or oxygen deficiency suppresses the structural distortion and static long-range antiferromagnetic order, therefore placing these materials into the same class of FeAs-based superconductors.

DOI: 10.1103/PhysRevB.78.132504 PACS number(s): 75.25.+z, 75.50.Ee, 25.40.Dn, 75.30.Fv

I. INTRODUCTION

The recent discovery of superconductivity in the rare-earth (R) iron-based superconductors $RFeAsO_{1-x}F_x$ (Refs. 1–4) and $A_{1-x}K_xFe_2As_2$ (A=Ba and Sr) (Refs. 5 and 6) has generated enormous interest because these materials are the first noncopper-oxide superconductors with T_c up to 55 K. All of the parent compounds ($RFeAsO$, R=La, Ce, and Nd; AFe_2As_2, A=Ba and Sr) of the iron-based superconductors investigated so far display a similar antiferromagnetic phase transition accompanying a tetragonal to orthorhombic structural distortion on cooling from 250 to 100 K.[7–18] Upon doping with fluorine, the long-range antiferromagnetic order is gradually suppressed before superconductivity appears, revealing a remarkably similar electronic phase diagram as that of the copper-oxide superconductors.[10,19] Although the lattice structure and magnetic properties of $RFeAsO_{1-x}F_x$ (R=La, Ce, Nd, and Pr) are similar, the maximum superconducting temperature T_c of doped $RFeAsO_{1-x}F_x$ is dramatically different increasing from ~26 to ~50 K when R changes from the nonmagnetic element La to magnetic elements Ce, Nd, and Pr. The sensitivity of the superconductivity to rare-earth substitution is really surprising since the RO layer is separated from the superconducting FeAs layer and does not directly control the electron-doping concentration. In order to understand why the rare-earth substitution affects the T_c, it is important to study how the rare-earth substitution affects the lattice and magnetic structures and the resulting electron-band structures.

In this Brief Report, we present neutron-scattering studies of the parent compound PrFeAsO and its superconducting counterpart $PrFeAsO_{1-x}F_x$, which possesses the highest T_c in the FeAs-based superconductor series.[20] Furthermore, since superconductivity in PrFeAsO can also be induced by forming oxygen vacancies, comparing the structure and magnetic properties of the F-doped and oxygen-deficient samples should provide some clues to understanding the role of doping in the FeAs-based class of superconductors. Here we investigate the structure and magnetic properties of the parent compound PrFeAsO and its superconducting counterparts $PrFeAsO_{0.85}F_{0.15}$ (T_c=52 K) and $PrFeAsO_{0.85}$ (T_c=52 K) by elastic neutron scattering. We find that PrFeAsO undergoes a structural distortion from tetragonal to orthorhombic symmetry near 153 K, accompanied by a magnetic transition to commensurate antiferromagnetic order of the Fe spins at ~127 K. These results, taken together with the observations of magnetic order in all the other systems which have been investigated to date,[8–18] demonstrate that the antiferromagnetic order is universal for the parent compounds of the FeAs-based superconductors. Upon 15% nominal F doping, both the structural distortion and magnetic order are suppressed identical to the other FeAs-based superconductors. We also find that the structural distortion and magnetic order are suppressed in the oxygen-deficient superconducting $PrFeAsO_{0.85}$ sample. Thus, removing oxygen from PrFeAsO has the same impact on the structural and magnetic properties as doping F in the system.

II. EXPERIMENTAL RESULTS AND DISCUSSION

We have employed neutron diffraction to study the structural and magnetic orders in polycrystalline samples of PrFeAsO, $PrFeAsO_{0.85}F_{0.15}$ (T_c=52 K), and $PrFeAsO_{0.85}$ (T_c=52 K). The samples were synthesized by a high-pressure method as described in Ref. 20. Our neutron-scattering experiments were carried out on the BT-1 powder diffractometer at the NIST Center for Neutron Research (NCNR) using the Ge(3,1,1) monochromator with an incident-beam wavelength of λ=2.0785 Å. The collimations before and after the monochromator and after the sample were 15′, 20′, and 7′ full width at half maximum (FWHM), respectively. Magnetic order parameters were taken on the HB-3 thermal triple-axis spectrometer at the High Flux Isotope Reactor, Oak Ridge National Laboratory with an incident-beam wavelength λ=2.36 Å with pyrolytic graphite (PG) (0,0,2) as monochromator and PG filters. Collimations

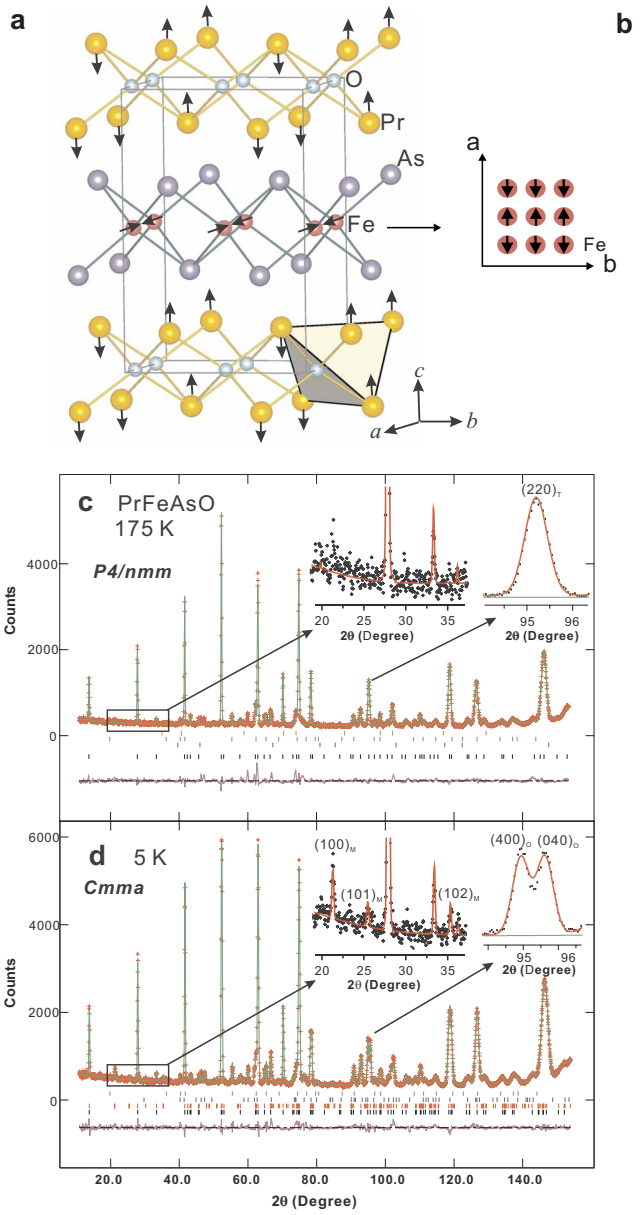

FIG. 1. (Color online) Lattice and magnetic structures in undoped PrFeAsO. (a) The three-dimensional antiferromagnetic structures of Fe as determined from the refinements of our neutron-diffraction data. (b) The magnetic structure of Fe in the FeAs plane. (c) Observed (crosses) and calculated (solid line) neutron-diffraction intensities of PrFeAsO at 175 K in the tetragonal structure with space group $P4/nmm$. The inset shows the detailed data for $18° < 2\theta < 38°$, where most of the observable magnetic peaks are located. 2θ is the diffraction angle, and the short vertical lines show the Bragg-peak positions. No magnetic peaks are observed at 175 K. The (purple) trace indicates the intensity difference between the observed and calculated structures. (d) Diffraction data at 5 K fitted with the orthorhombic structure of space group *Cmma*. The inset plots the detailed data in $18° < 2\theta < 38°$ showing three indexed magnetic peaks at 5 K along with the observed splitting of the structural peak. The magnetic peaks are accounted for by the combined contributions of Fe and Pr. The (1,0,0) peak vanishes completely above the Pr Néel temperature of 14 K, while the (1,0,1) and (1,0,2) peaks persist above 14 K and vanish at 127 K as shown in Fig. 2(b).

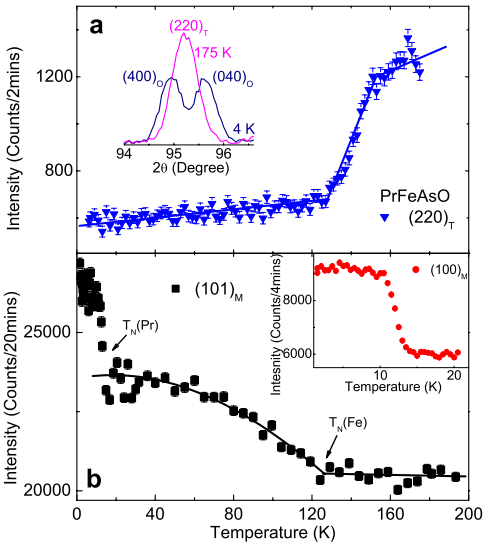

FIG. 2. (Color online) Temperature dependence of $(2,2,0)_T$ nuclear Bragg peak and magnetic $(1,0,0)_M$ and $(1,0,1)_M$ peaks. The data in (a) and (b) are collected on BT-1 and HB-3, respectively. (a) Temperature dependence of the $(2,2,0)_T$ (T denotes tetragonal) nuclear Bragg peak showing that the onset of the structure phase transition is about 153 K. The inset shows the $(2,2,0)_T$ reflection above and below the transition temperature. (b) Temperature dependence of the order parameter for the $(1,0,1)_M$ (M denotes magnetic) magnetic Bragg peak. The large increase in the intensity below 14 K is due to Pr ordering as confirmed by the temperature dependence of the $(1,0,0)_M$ magnetic Bragg peak, which has only an intensity contribution from Pr. The intensity of the $(1,0,1)_M$ peak vanishes at the Néel temperature of 127 K for the iron-spin ordering.

in these configurations were coarse (typically ~40–50′) for intensity reasons.

Our high-resolution measurements on BT-1 show that the high-temperature structure (175 K) in PrFeAsO can be well described by the expected tetragonal structure of space group $P4/nmm$ [Fig. 1(c)]. The refined structural parameters are listed in Table Ia . Figure 1(d) shows the low-temperature (5 K) diffraction pattern and refinement profiles for PrFeAsO, which can be described with the orthorhombic structure of space group *Cmma*. The orthorhombic distortion splits the $(220)_T$ Bragg peak of the tetragonal structure into two peaks, $(400)_O$ and $(040)_O$ in the orthorhombic structure, as shown in the inset of Fig. 2(a). The insets of Figs. 1(c) and 1(d) show the details of the diffraction pattern for 2θ between 20° and 37°, where most of the observable magnetic peaks are located. We can clearly see several magnetic peaks at 5 K, which can be simply indexed with the expected commensurate magnetic structure. These peaks are absent in the 175 K diffraction pattern indicating that the system is in the paramagnetic state at this temperature. Refinements using the GSAS program give excellent fits for the low-temperature diffraction pattern, where the magnetic peaks are well accounted for by the combined Pr and Fe antiferromagnetic orders as shown in Figs. 1(a) and 1(b). The Fe magnetic unit cell can be indexed as $\sqrt{2}a_N\sqrt{2}b_Nc_N$, which is exactly the same as for CeFeAsO.[10] The Fe spins order antiferromagnetically along the orthorhombic a axis and ferromagneti-

TABLE I. Ia. Refined structural parameters of $PrFeAsO_{1-x}F_x$ with $x=0$ at 175 K and $x=0.16$ at 5 K and $PrFeAsO_{0.85}$ at 5 K. Space group: $P4/nmm$, where PrFeAsO with $a=3.977\ 16(5)$, $c=8.6057(2)$Å; $PrFeAsO_{0.85}F_{0.15}$ with $a=3.9700(1)$, $c=8.5331(4)$ Å; and $PrFeAsO_{0.85}$ with $a=3.9686(1)$, $c=8.5365(3)$ Å. PrFeAsO with $R_p=4.55\%$, $w_{R_p}=5.8\%$, and $\chi^2=1.387$; $PrFeAsO_{0.85}F_{0.15}$ with $R_p=8.24\%$, $w_{R_p}=10.62\%$, and $\chi^2=3.635$; and $PrFeAsO_{0.85}$ with $R_p=6.99\%$, $w_{R_p}=9.23\%$, and $\chi^2=4.652$. (b) Refined structural parameters of PrFeAsO at 5 K. Space group: *Cmma*, where $a=5.6374(1)$, $b=5.6063(1)$, and $c=8.5966(2)$ Å. $R_p=4.22\%$, $w_{R_p}=5.73\%$, and $\chi^2=2.180$.

(a)

Atom	Site	x	y	z(PrFeAsO)/B (Å^2)	z($PrFeAsO_{0.85}F_{0.15}$)/B (Å^2)	z($PrFeAsO_{0.85}$)/B (Å^2)	n(O)
Pr	2*c*	$\frac{1}{4}$	$\frac{1}{4}$	0.1397(6)/0.89(9)	0.1504(1)/0.5(1)	0.1450(7)/0.4(1)	
Fe	2*b*	$\frac{3}{4}$	$\frac{1}{4}$	$\frac{1}{2}$ /0.65(4)	$\frac{1}{2}$ /0.46(6)	$\frac{1}{2}$ /0.30(5)	
As	2*c*	$\frac{1}{4}$	$\frac{1}{4}$	0.6559(4)/0.74(6)	0.6548(5)/0.46(6)	0.6546(5)/0.75(9)	
O/F	2*a*	$\frac{3}{4}$	$\frac{1}{4}$	0/0.63(6)	0/0.8(1)	0/0.791)	0.92(1)

(b)

Atom	Site	x	y	z	B (Å^2)	M_x (μ_B)	M_y (μ_B)	M_z (μ_B)
Pr	4*g*	0	$\frac{1}{4}$	0.1385(5)	0.96(7)	0	0	0.84(4)
Fe	4*b*	$\frac{1}{4}$	0	$\frac{1}{2}$	0.44(4)	0.48(9)	0	0
As	4*g*	0	$\frac{1}{4}$	0.6565(3)	0.71(6)			
O	4*a*	$\frac{1}{4}$	0	0	0.77(6)			

cally along the *b* and *c* axes with the moment direction along the *a* axis. The measured static-ordered Fe moment is 0.48(9) μ_B at 5 K, where numbers in parentheses indicate one standard deviation statistical uncertainty in the last decimal place, and μ_B denotes the Bohr magneton. Error bars in this Brief Report also represent one standard deviation.

Figure 2 plots the order-parameter data for the structural and magnetic phase transitions. The onset of the structural transition is indicated by the initial drop in the $(220)_T$ peak intensity with temperature, which is observed to be around 153 K [Fig. 2(a)]. Figure 2(b) reveals that the Pr Néel temperature is about 14 K, while the Fe Néel temperature is about 127 K. The Pr spins align along the *c* axis with the rather complicated magnetic structure shown in Fig. 1(a), where trios of spins are coupled ferromagnetically, while adjacent trios align antiferromagnetically. The ordered moment in the ground state is 0.84(4) μ_B at 5 K (see Table Ib). Compared to the undoped PrFeAsO system, there is no observable orthorhombic structure distortion in the $PrFeAsO_{0.85}F_{0.15}$ down to 5 K [Fig. 3(a)]. The tetragonal $P4/nmm$ structure can describe the diffraction pattern very well, as is the case for all the other highly doped FeAs-based superconductors. The oxygen-deficient $PrFeAsO_{0.85}$ sample also has no orthorhombic structural distortion down to 5 K, and the refined structural parameters are essentially the same as for the F-doped sample (Table Ib) [Fig. 1(c)]. In addition, neither $PrFeAsO_{0.85}F_{0.15}$ nor $PrFeAsO_{0.85}$ has any observable magnetic order at 5 K suggesting that antiferromagnetic order is directly competing with superconductivity. Note that in the GSAS refinements for PrFeAsO, $PrFeAsO_{0.85}F_{0.15}$, and $PrFeAsO_{0.85}$, we assumed that oxygen, fluorine, and oxygen deficiencies are at their nominal values. As one can clearly see impurity scattering in the fitted diffraction patterns in

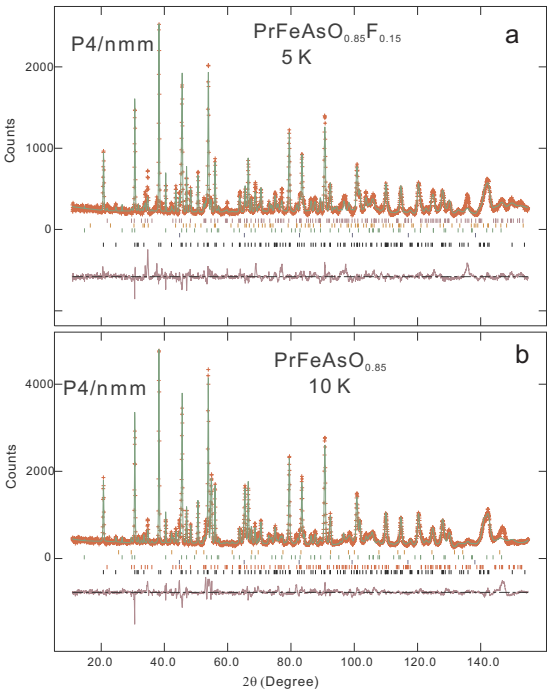

FIG. 3. (Color online) Structural diffraction data for the $PrFeAsO_{0.85}F_{0.15}$ and $PrFeAsO_{0.85}$ superconducting samples. The data were collected on the BT-1 diffractometer. (a) Observed (crosses) and calculated (solid line) neutron-diffraction intensities of $PrFeAsO_{0.85}F_{0.15}$ at 5 K for the tetragonal structure (space group $P4/nmm$). The short vertical lines show the Bragg-peak positions. The (purple/gray) trace indicates the intensity difference between the observed and calculated structures. (b) Observed (crosses) and calculated (solid line) neutron-diffraction intensities of $PrFeAsO_{0.85}$ at 5 K refined with the tetragonal space group $P4/nmm$.

Figs. 1 and 3, such an assumption may not be accurate. However, since the actual oxygen, fluorine, and oxygen deficiencies are difficult to control and determine,[1–4] and we are only interested in knowing whether the observed magnetic structure can survive superconductivity, this assumption is likely to be adequate. In fact, for both the fluorine-doped and oxygen-deficient superconducting samples, the actual electron-doping levels are presently unknown. As a consequence, it is unclear why they have similar superconducting transition temperatures even though F substitution should have different electron-doping effect from oxygen deficiency in *R*FeAsO-based superconductors.

III. CONCLUSIONS

In summary, we have carried out detailed neutron-scattering studies of the magnetic and nuclear structures of the FeAs-based superconductors $PrFeAsO_{0.85}F_{0.15}$ (T_c =52 K) and $PrFeAsO_{0.85}$ (T_c=52 K) along with their parent compound PrFeAsO. Very similar to the other parent compounds of the FeAs-based superconductors, PrFeAsO has a simple collinear antiferromagnetic structure of the iron spins with a Néel temperature of 127 K and an ordered moment of 0.48(9) μ_B. The magnetic structure is identical to that of CeFeAsO (Ref. 10) but does not have the *c* axis unit-cell doubling like that of LaFeAsO (Ref. 8). The magnetic moments on the Pr sites are also antiferromagnetically ordered below 14 K, similar to the parent compounds of the other rare-earth FeAs-based superconductors such as CeFeAsO (Ref. 10) and NdFeAsO.[12] The Pr spins align along the *c* axis with a magnetic structure where trios of spins are coupled ferromagnetically, while adjacent trios align antiferromagnetically. The ordered moment in the ground state is 0.84(4) μ_B at 5 K. The iron magnetic order occurs below the transition from the high-temperature tetragonal phase to the low-temperature orthorhombic phase of the parent compound that occurs around 153 K. The structural distortion and iron antiferromagnetic order are suppressed completely in the optimally doped superconducting samples regardless of whether the superconducting state is achieved by F doping or oxygen vacancies, and the two types of doping yield very similar crystallographic structures.

Note added. Upon finishing the present Brief Report, we became aware of a similar neutron powder-diffraction work on PrFeAsO and $PrFeAsO_{1-x}F_x$ (Ref. 21).

ACKNOWLEDGMENTS

This work was supported by the U.S. National Science Foundation through Grant No. DMR-0756568 and by the Division of Materials Science, Basic Energy Sciences, U.S. Department of Energy through Grant No. DOE DE-FG02-05ER46202. This work was also supported in part by the Division of Scientific User Facilities, Basic Energy Sciences, U.S. Department of Energy. The work at the Institute of Physics, Chinese Academy of Sciences was supported by the National Science Foundation of China, the Chinese Academy of Sciences, and the Ministry of Science and Technology of China. The work at the Institute of Physics was also supported in part by Chinese Academy of Science Projects ITSNEM No. 2006CB601000 and No. 2006CB92180.

[1] Y. Kamihara *et al.*, J. Am. Chem. Soc. **130**, 3296 (2008).
[2] X. H. Chen *et al.*, Nature (London) **453**, 761 (2008).
[3] G. F. Chen *et al.*, Phys. Rev. Lett. **100**, 247002 (2008).
[4] Zhi-An Ren *et al.*, Europhys. Lett. **83**, 17002 (2008).
[5] M. Rotter, M. Tegel, and D. Johrendt, , Phys. Rev. Lett. **101**, 107006 (2008).
[6] G. F. Chen, Z. Li, G. Li, W. Z. Hu, J. Dong, X. D. Zhang, P. L. Wang, and J. L. Luo, Chin. Phys. Lett. **25**, 3403 (2008).
[7] J. Dong *et al.*, Europhys. Lett. **83**, 27006 (2008).
[8] C. de la Cruz *et al.*, Nature (London) **453**, 899 (2008).
[9] H. H. Klauss *et al.*, Phys. Rev. Lett. **101**, 077005 (2008).
[10] Jun Zhao *et al.*, arXiv:0806.2528, Nature Materials (to be published).
[11] M. A. McGuire *et al.*, Phys. Rev. B **78**, 094517 (2008).
[12] Y. Chen *et al.*, Phys. Rev. B **78**, 064515 (2008).
[13] Q. Huang *et al.*, arXiv:0806.2776 (unpublished).
[14] Jun Zhao *et al.*, Phys. Rev. B **78**, 140504 (2008).
[15] A. I. Goldman *et al.*, Phys. Rev. B **78**, 100506 (2008).
[16] S. Kitao *et al.*, arXiv:0805.0041 (unpublished).
[17] J. P. Carlo *et al.*, arXiv:0805.2186 (unpublished).
[18] J. Drew *et al.*, Phys. Rev. B **101**, 097010 (2008).
[19] J. M. Tranquada *et al.*, Phys. Rev. B **38**, 2477 (1988).
[20] Z. A. Ren *et al.*, Mater. Res. Innovations **12**, 105 (2008).
[21] S. A. Kimber *et al.*, arXiv:0807.4441, Phys. Rev. B (to be published).